© 2014. Published by The Company of Biologists Ltd | Development (2014) 141, 4580-4589 doi:10.1242/dev.111229

RESEARCH ARTICLE

The *Arabidopsis* Mediator CDK8 module genes *CCT* (*MED12*) and *GCT* (*MED13*) are global regulators of developmental phase transitions

C. Stewart Gillmor[1,2,*], Claudia O. Silva-Ortega[1], Matthew R. Willmann[2], Manuel Buendía-Monreal[1] and R. Scott Poethig[2,*]

ABSTRACT

Temporal coordination of developmental programs is necessary for normal ontogeny, but the mechanism by which this is accomplished is still poorly understood. We have previously shown that two components of the Mediator CDK8 module encoded by *CENTER CITY* (*CCT*; *Arabidopsis MED12*) and *GRAND CENTRAL* (*GCT*; *Arabidopsis MED13*) are required for timing of pattern formation during embryogenesis. A morphological, molecular and genomic analysis of the post-embryonic phenotype of *gct* and *cct* mutants demonstrated that these genes also promote at least three subsequent developmental transitions: germination, vegetative phase change, and flowering. Genetic and molecular analyses indicate that *GCT* and *CCT* operate in parallel to gibberellic acid, a phytohormone known to regulate these same three transitions. We demonstrate that the delay in vegetative phase change in *gct* and *cct* is largely due to overexpression of miR156, and that the delay in flowering is due in part to upregulation of *FLC*. Thus, *GCT* and *CCT* coordinate vegetative and floral transitions by repressing the repressors miR156 and *FLC*. Our results suggest that MED12 and MED13 act as global regulators of developmental timing by fine-tuning the expression of temporal regulatory genes.

KEY WORDS: miR156, *FLC*, MED12, MED13, Mediator, *Arabidopsis thaliana*

INTRODUCTION

Temporal coordination of developmental programs underlies many processes in plants and animals and plays a major role in evolution. For example, it is hypothesized that an extended phase of rapid brain growth (a characteristic of juvenile development) played a key role in the evolution of humans from their primate ancestors (Gould, 1977). In flowering plants, changes in the relative timing of juvenile and adult development can have major effects on traits such as leaf morphology and the onset of flowering (reviewed by Huijser and Schmid, 2011; Geuten and Coenen, 2013; Poethig, 2013). Resistance to herbivory, as well as changes in cell wall composition, also have an important temporal component (Abedon et al., 2006; reviewed by Boege and Marquis, 2005 and Chandler et al., 2011). Thus, the study of developmental timing is crucial to our understanding of plant and animal ontogeny, physiology and evolution.

Post-embryonic phases of plant development include germination, seedling growth, the juvenile and adult vegetative phases, and flowering. Transitions between some of these programs are abrupt, whereas other transitions are more gradual. For example, germination entails a drastic switch from dormancy and growth repression (seed) to active growth and metabolism (seedling) (Bassel et al., 2011). By contrast, gradual transitions occur during the transition from the juvenile to the adult vegetative phase: aspects such as shape, serrations and epidermal hairs change incrementally between successive leaves. Depending on the species, leaf morphological traits may become either more or less complex from the juvenile to adult vegetative phase, when plants become reproductively competent (Poethig, 2013). The reproductive transition is relatively rapid, as the shoot apical meristem changes from leaf initiation to producing branches and flowers (Amasino, 2010).

Studies of the model plants *Arabidopsis* and maize have been particularly important in elucidating some of the molecular mechanisms that regulate phase-specific developmental programs, and have implicated factors such as the phytohormone gibberellic acid (GA), microRNAs (miRNAs) and epigenetic marks in the regulation of genes involved in these processes. The role of GA in promoting developmental transitions in plants is well established. GA activates seed germination, when rapid cell elongation is required for the embryo to rupture the seed coat, and simultaneously represses the expression of seed-specific genes (Koornneef and van der Veen, 1980; Ogas et al., 1997). GA also promotes leaf expansion during vegetative growth, as well as the onset of adult epidermal characteristics such as trichomes, which are canonical markers of vegetative phase change in *Arabidopsis* and maize (Evans and Poethig, 1995; Telfer et al., 1997). In addition, GA is required for the transition from vegetative growth to flowering (Wilson et al., 1992; Yu et al., 2012). Similarly, epigenetic regulation of gene expression, in particular through Histone 3 lysine 27 (H3K27) methylation, is important for both the seed-to-seedling and vegetative-to-reproductive transitions in plants (reviewed by Crevillén and Dean, 2011). Loss of H3K27 methylation affects the embryo-to-seedling transition by increasing dormancy and causing expression of seed-specific genes in seedlings (Bouyer et al., 2011; Zhang et al., 2008), while decreased H3K27 methylation at the floral repressor *FLOWERING LOCUS C* (*FLC*) delays flowering (Bastow et al., 2004).

Another important temporal regulator in plants is miR156 (Poethig, 2013), which regulates leaf traits and flowering by repressing members of the SPL family of transcription factors. SPL proteins positively regulate the expression of miR172, which in turn represses AP2-like transcription factors that inhibit flowering

[1]Laboratorio Nacional de Genómica para la Biodiversidad (Langebio), Unidad de Genómica Avanzada, Centro de Investigación y de Estudios Avanzados del Instituto Politécnico Nacional (CINVESTAV-IPN), Irapuato, Guanajuato, 36821, Mexico. [2]Department of Biology, University of Pennsylvania, Philadelphia, PA 19104, USA.

*Authors for correspondence (sgillmor@langebio.cinvestav.mx; spoethig@sas.upenn.edu)

Received 10 April 2014; Accepted 21 September 2014

Development (2014) 141, 4580-4589 doi:10.1242/dev.111229

(Aukerman and Sakai, 2003; Chuck et al., 2007; Wu and Poethig, 2006; Wu et al., 2009; Wang et al., 2009). It has recently been shown that miR156 exerts its effects on flowering in parallel with GA because GA induces degradation of DELLA repressor proteins that are bound to SPL transcription factors (Yu et al., 2012). miR156 is abundant in seedlings, and decreases during vegetative development, partly due to transcriptional repression by leaf-derived sugars (Wu and Poethig, 2006; Yang et al., 2011, 2013; Yu et al., 2013). However, miR156 levels decrease during vegetative development even in the absence of sugar signaling, indicating that there are additional, as yet unknown, factors that regulate miR156 abundance during vegetative development (Yang et al., 2013).

The transcriptional co-activator Mediator has recently emerged as a key integrator of signaling pathways during development in both animals and plants, capable of influencing RNA polymerase II transcription of mRNAs and miRNAs at all stages of the transcription process, including through epigenetic regulation (Kim et al., 2011; reviewed by Yin and Wang, 2014). Mediator is a large protein complex that is conserved in all eukaryotes and has two major components: Core Mediator, which acts as a transcriptional co-activator, and the Cyclin Dependent Kinase 8 (CDK8) module, which represses transcription by modulating the activity of Core Mediator (Bourbon, 2008; reviewed by Carlsten et al., 2013). The CDK8 module is usually thought of as a transcriptional repressor, since the active form of Core Mediator is never purified together with the CDK8 module (Carlsten et al., 2013); however, in some contexts, the CDK8 module can also act to stimulate transcription, usually through the kinase activity of the CDK8 protein on the C-terminal domain of RNA polymerase II (reviewed by Nemet et al., 2013).

Mediator is capable of integrating diverse signaling inputs to influence transcription of multiple genes. For example, the MED18 subunit of *Arabidopsis* Core Mediator regulates fungal resistance, responses to the phytohormone abscisic acid, and flowering time, by influencing transcription initiation, elongation and termination, as well as RNA polymerase II occupancy and deposition of Histone 3 lysine 36 (H3K36) methylation (Lai et al., 2014). Likewise, studies in yeast and humans have shown that the CDK8 module can inhibit transcription through different mechanisms, including preventing physical association of Core Mediator with RNA polymerase II, and recruiting Histone 3 lysine 9 (H3K9) and H3K27 methylation at target genes (Tsai et al., 2013; Ding et al., 2008; Chaturvedi et al., 2012). The CDK8 module is composed of CDK8, Cyclin C, MED12 and MED13 (Carlsten et al., 2013). In *Arabidopsis*, MED12 is encoded by *CENTER CITY* [*CCT*; also known as *CRYPTIC PRECOCIOUS* (*CRP*)], MED13 is encoded by *GRAND CENTRAL* [*GCT*; also known as *MACCHI-BOU 2* (*MAB2*)] and CDK8 is encoded by *HUA ENHANCER 3* (*HEN3*) (Gillmor et al., 2010; Imura et al., 2012; Ito et al., 2011; Wang and Chen, 2004). *CCT* and *GCT* have previously been implicated in temporal regulation of development, as *gct* and *cct* mutants affect the timing of radial pattern formation during early embryogenesis (Gillmor et al., 2010).

Here, we demonstrate that *GCT* and *CCT* are global regulators of developmental transitions, promoting the embryo-to-seedling, juvenile-to-adult and vegetative-to-reproductive transitions. We show that one of the most important post-embryonic roles of *GCT* and *CCT* is to repress seed-specific transcripts in seedlings, and to promote growth after germination. In addition, we demonstrate that *GCT* and *CCT* regulate the abundance of miR156 during vegetative development, and that the upregulation of miR156 in *gct* and *cct* plants plays a major role in extending the vegetative phase in these mutants. *GCT* and *CCT* also regulate levels of *FLC*, and overexpression of *FLC* is responsible for much of the delayed flowering phenotype in *gct* and *cct* mutants. Thus, *CCT* and *GCT* act as master regulators of developmental transitions during the plant life cycle by repressing the expression of key temporal control genes.

RESULTS

GCT and *CCT* are required for post-embryonic development

gct and *cct* mutants germinate well, but develop abnormally following germination (99.5% germination in progeny of *gct*/+, *n*=428; 99.1% germination in progeny of *cct*/+, *n*=441). Although loss-of-function mutations of both genes are fully penetrant, they display variable expressivity: some mutant seedlings have small leaves, short petioles and malformed cotyledons but continue to grow and develop (we refer to this as the 'grow' phenotype), whereas others germinate and produce a root, but do not form leaf primordia and arrest at this stage (we refer to this as the 'arrest' phenotype) (Fig. 1B,C). 54% of *gct* seedlings and 24% of *cct* seedlings display the arrest phenotype. This variable expressivity is not attributable to partial activity of the mutant gene products: all five alleles of *gct* and all three alleles of *cct* described by Gillmor et al. (2010) generate both grow and arrest phenotypes (data not shown). These *gct* and *cct* alleles include both RNA nulls and predicted functional nulls (supplementary material Fig. S1) (Ito et al., 2011; Imura et al., 2012). Taken together, these molecular and functional data demonstrate that null mutants for each gene produce both grow and arrest phenotypes.

Analysis of *GCT* and *CCT* expression in a public dataset revealed that both genes are broadly expressed at low levels throughout post-embryonic development (supplementary material Fig. S2) (Schmid et al., 2005; Winter et al., 2007). The functional relationship between *GCT* and *CCT* was investigated by constructing plants mutant for both genes. The genotypes of the phenotypically mutant progeny of a self-pollinated *gct*/+ *cct*/+ plant were determined using allele-specific molecular markers. No double mutants were identified among the 27 plants with the grow phenotype, but 3 out of 18 plants with the arrest phenotype were homozygous for

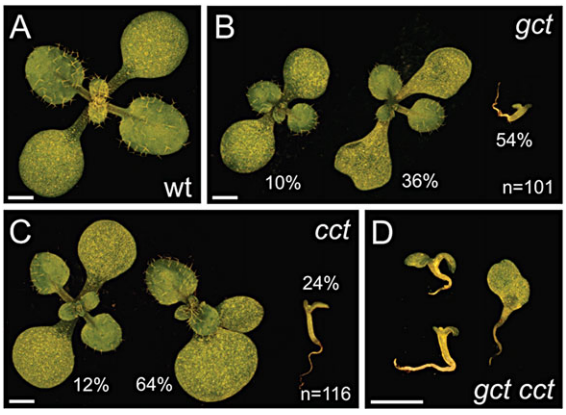

Fig. 1. *GCT* and *CCT* act together to promote post-embryonic growth. Wild-type (wt), *gct* and *cct Arabidopsis thaliana* seedlings after 10 d of growth on soil. (A) Wt seedling. (B) Phenotypic spectrum of *gct* seedlings: 10% showed regularly shaped cotyledons, 36% showed irregularly shaped cotyledons, and 54% arrested growth. (C) Phenotypic spectrum of *cct* seedlings: 12% showed regularly shaped cotyledons, 64% showed irregularly shaped cotyledons, and 24% arrested growth. (D) *gct cct* double-mutant seedlings show 100% expressivity of the arrested growth phenotype. Scale bars: 1 mm.

Development (2014) 141, 4580-4589 doi:10.1242/dev.111229

both mutations; the phenotypes of these *gct cct* double mutants are shown in Fig. 1D. *GCT* and *CCT* are not linked, so the expected frequency of double mutants among progeny displaying a mutant phenotype is 1/7; the ratio of double mutants (0/27) among grow phenotype seedlings is significantly different from this ratio (χ^2 goodness of fit test, P=0.03), whereas the frequency of double mutants among arrest phenotype seedlings (3/18) is not significantly different from this ratio. We conclude that loss of both *GCT* and *CCT* consistently leads to growth arrest. These results, as well as the phenotypic similarity of *gct* and *cct* mutations, suggest that these genes operate together or in parallel to regulate a core set of processes required for post-embryonic development.

Genes misregulated in both *gct* and *cct* seedlings demonstrate a role for *GCT* and *CCT* in developmental transitions

To investigate the molecular basis for the post-embryonic phenotype of *gct* and *cct*, and the vegetative and reproductive changes described below, we used Affymetrix microarrays to compare steady-state mRNA levels in 7-day-old (7 d) wild-type (wt) seedlings and 9 d *gct* and *cct* seedlings, when the first two leaf primordia of these three genotypes were 1 mm in length (Fig. 2A). Compared with wt, transcripts for 1267 probe sets were more abundant in *gct* and 1373 were less abundant in *gct* (supplementary material Table S2), whereas transcripts for 925 probe sets were more abundant in *cct* and 1051 were less abundant in *cct* (supplementary material Table S3) (Limma, with a Benjamini-Hochberg adjustment, P<0.05). In total, 490 probe sets increased and 683 decreased in both *gct* and *cct* (supplementary material Table S4), an overlap that is greater than would be expected by chance (Fisher's exact test, P=0). Thus, *GCT* and *CCT* share a large, but not totally overlapping, set of direct and indirect gene targets.

An analysis of genes with transcripts that increase or decrease in both *gct* and *cct* is presented in supplementary material Table S5. These enriched terms (including GO terms) suggest a role for *GCT* and *CCT* in a number of growth-related processes, including the secretory pathway (such as GPI-anchored proteins and N-linked glycosylation), and cell wall remodeling. Among the most highly overrepresented GO terms were those related to seed-specific processes and flowering (supplementary material Table S5). An inspection of the genes that are most highly overexpressed in both *gct* and *cct* revealed many seed-specific transcripts, as well as the flowering repressor *FLC*; flowering genes that showed significant decreases in expression included *FLOWERING LOCUS T* (*FT*) and

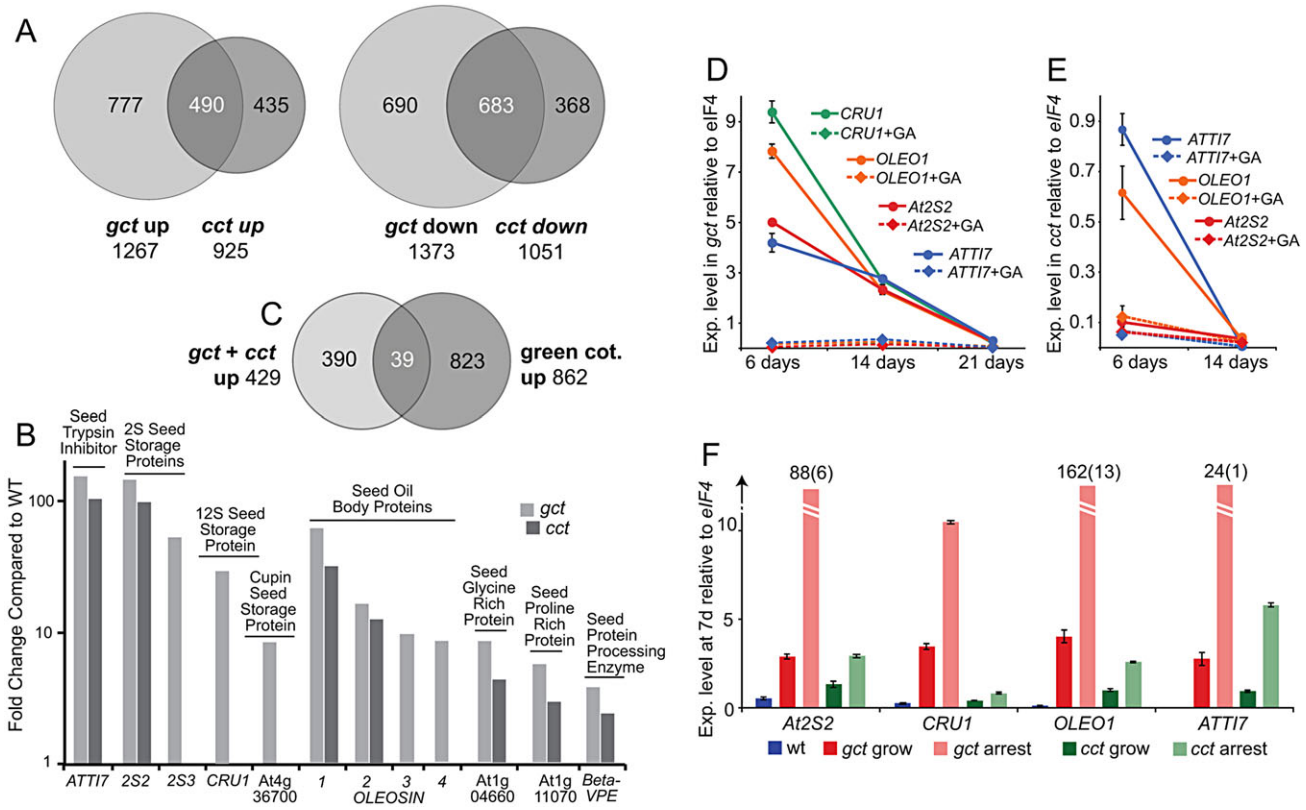

Fig. 2. *GCT* and *CCT* have many common targets and repress embryo-specific genes in seedlings. Microarray and qRT-PCR analyses of gene expression in wt, *gct* and *cct* seedlings. (A) Affymetrix microarray analysis of genes that change in 9 d *gct* and *cct* seedlings compared with 7 d wt (P<0.05). Shown is the number of genes that change in *gct* only (light gray circle), in *cct* only (medium gray circle) or in both (overlap), with the total number of genes that change in these mutants shown beneath. Three biological replicates were performed.16,826 non-control probe sets were present in at least three of the nine microarrays. Fisher's exact test, P=0 for significance of overlap of genes that increase or decrease in both *gct* and *cct*. (B) Affymetrix microarray data for seed-specific genes that are heterochronically misexpressed in *gct* and *cct* seedlings. Log_{10} scale. (C) Comparison of transcripts that are upregulated in both *gct* and *cct* (light gray) with transcripts upregulated from the torpedo to green cotyledon stage from Willmann et al. (2011) (medium gray); intersection shows the number of transcripts upregulated in both. 15,449 probe sets were present in both samples. Fisher's exact test, $P=1.6\times10^{-4}$ for significance of overlap of the two gene sets. (D,E) qRT-PCR validation of seed-specific genes expressed in *gct* seedlings at 6 d, 14 d and 21 d or in *cct* seedlings at 6 d and 14 d (solid lines); GA_3 treatment reduces the expression of these genes to negligible levels (dashed lines). (F) qRT-PCR expression analysis of seed-specific genes in 7 d wt seedlings, *gct* seedlings that grow or arrest, and *cct* seedlings that grow or arrest. For qRT-PCR experiments, the average and s.d. of three technical replicates for one representative experiment of two biological replicates is shown.

Development (2014) 141, 4580-4589 doi:10.1242/dev.111229

SUPPRESSOR OF CONSTANS 1 (*SOC1*) (both of which are repressed by *FLC*), as well as *CONSTANS* (*CO*) (supplementary material Table S4). These results suggest that, in addition to controlling the timing of embryonic development (Gillmor et al., 2010), *GCT* and *CCT* regulate post-embryonic developmental transitions.

GCT and *CCT* promote the transition to post-embryonic development by repressing the expression of embryo-specific genes after germination

As mentioned above, a number of seed-specific transcripts were among the most highly overexpressed genes in both *gct* and *cct* seedlings (Fig. 2B; supplementary material Table S4). In support of a role for *GCT* and *CCT* in regulating the seed-to-seedling transition, we found a significant overlap between probe sets upregulated in both *gct* and *cct* and those increasing at the green cotyledon stage of embryogenesis (Fig. 2C; Fisher's exact test right-tail, $P \leq 1.61 \times 10^{-4}$) (Willmann et al., 2011). Thus, *gct* and *cct* seedlings show molecular signatures of late embryogenesis.

To confirm and extend these results, we used qRT-PCR to measure the abundance of four seed-specific transcripts (*At2S2*, *CRU1*, *OLEO1*, *ATTI7*) in 6 d, 14 d and 21 d wt and mutant plants; only mutant plants with the grow phenotype were used for this experiment. All four genes were expressed at high levels in 6 d *gct* seedlings, and their expression declined gradually in this mutant over the next 2 weeks (Fig. 2D). *At2S2*, *OLEO1* and *ATTI7* were also misexpressed in 6 d *cct* seedlings, but were much less elevated than in *gct* (Fig. 2E) and also disappeared faster in this genotype. Consistent with the results of the microarray analysis, *CRU1* was unaffected by *cct*. We also compared the expression of these genes in 7 d *gct* and *cct* seedlings with the grow and arrest phenotypes (Fig. 2F). In every case, these genes were expressed at significantly higher levels in seedlings with the arrest phenotype. For example, *At2S2* was elevated 3-fold in grow *gct* seedlings and 88-fold in arrest *gct* seedlings, while *OLEO1* was elevated 4-fold in grow *gct* seedlings and 162-fold in arrest *gct* seedlings. These results demonstrate that *GCT* and *CCT* repress the expression of embryo-specific genes during post-embryonic development.

The phytohormone GA has a similar function to GCT and CCT in that it promotes seed germination and represses embryonic identity in young seedlings (Koornneef and van der Veen, 1980; Ogas et al., 1997). To determine if GA operates via *GCT* and *CCT*, we examined the effect of this hormone on the expression of *At2S2*, *CRU1*, *OLEO1*, *ATTI7* in *gct* and *cct* mutants. These genes were strongly repressed by GA in both mutants (Fig. 2D,E), indicating that GA represses embryonic gene expression independently of *GCT* and *CCT*.

GCT and *CCT* promote vegetative phase change by repressing miR156

In *Arabidopsis*, the transition from the juvenile to the adult phase of vegetative development is marked by changes in leaf shape (round to elongated), leaf serration (smooth to serrated) and abaxial trichome production (absent to present) (Röbbelen, 1957; Chien and Sussex, 1996; Telfer et al., 1997). *gct* and *cct* delayed the appearance of the adult forms of all of these traits (Fig. 3). In long-day conditions, *gct* and *cct* plants had over twice as many leaves without abaxial trichomes as wt plants (Table 1). *gct* and *cct* also

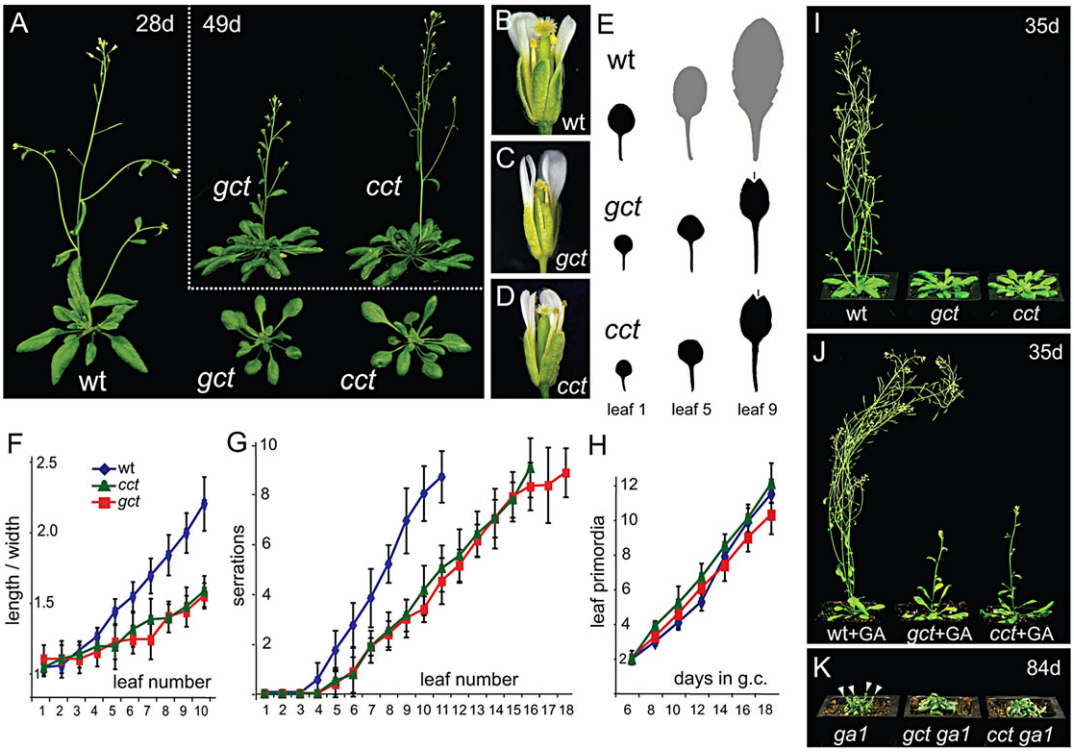

Fig. 3. *gct* and *cct* mutations delay the expression of adult leaf traits and the transition to flowering. (A) Wt, *gct* and *cct* plants after 28 d of growth and *gct* and *cct* after 49 d of growth (inset) in long-day conditions. (B) Wt flower at anthesis. (C) *gct* flower, no viable pollen is produced. (D) *cct* flower, almost no viable pollen is produced. (E) Silhouettes of fully expanded leaves of wt, *gct* and *cct*. Breaks at the distal end of *gct* and *cct* leaves (marked by short lines) are due to flattening of convex leaves for scanning. (F) Length-to-width ratios for the first ten leaves of wt, *gct* and *cct*. (G) Number of serrations per leaf for wt, *gct* and *cct*. (H) Rate of leaf initiation in wt, *gct* and *cct*. Error bars (F-H) represent s.d. ($n \geq 8$). (I,J) 35 d wt, *gct* and *cct* plants with (J) and without (I) daily GA_3 treatment. (K) 84 d *ga1-3*, *gct ga1-3* and *cct ga1-3* plants. Arrowheads point to inflorescences.

Development (2014) 141, 4580-4589 doi:10.1242/dev.111229

Table 1. Leaf identity and flowering time data for wt, *gct*, *cct* in *flc-3* and *ga1-3* backgrounds or with GA_3 treatment

Genotype/treatment	Leaves without abaxial trichomes	Leaves with abaxial trichomes	Bracts	Days to first open flower	*n*
wt Col	4.9 (0.3)	4.8 (0.7)	3.1 (0.3)	24.7 (1.0)	10
gct	12.9 (0.9)	18.9 (3.9)	7.2 (1.2)	50.8 (5.0)	17
cct	11.6 (1.4)	13.2 (2.0)	7.8 (1.6)	41.3 (3.7)	15
wt Col+GA	2.0 (0.0)	4.2 (0.6)	3.5 (0.6)	18.5 (0.8)	12
gct+GA	5.5 (0.8)	6.2 (0.8)	12.1 (2)	32.3 (3.1)	10
cct+GA	4.8 (0.7)	5.1 (0.6)	12.5 (1.7)	31.4 (2.4)	10
ga1-3	>20	3 (2)	n.d.	70 (2)	11
gct ga1-3	>30	0	n.d.	>105	5
cct ga1-3	>30	0	n.d.	>91	13
flc-3	4.5 (0.6)	3.8 (0.8)	2.8 (0.5)	23.7 (0.9)	28
gct flc-3	12.6 (1.5)	9.1 (1.6)	5.4 (0.7)	43.2 (0.7)	15
cct flc-3	10.1 (1.0)	9.1 (2.1)	5.8 (1.4)	35.2 (2.4)	21

Plants were grown in long-day conditions. s.d. is shown in parentheses.
+GA, daily treatment with 100 µM GA_3.
n.d., not determined.

had rounder leaves than wt (Fig. 3E,F) and began to produce serrated leaves later and with a slower rate of increase in serration number than wt plants (Fig. 3E,G). Importantly, the rate of leaf initiation was almost identical in wt, *gct* and *cct*, indicating that the increased number of juvenile leaves in *gct* and *cct* is not due to an increase in the rate of leaf production (Fig. 3H).

The phytohormone GA promotes several of the processes regulated by *GCT* and *CCT*, including the onset of abaxial trichome production and the transition to flowering (Chien and Sussex, 1996; Telfer et al., 1997; Wilson et al., 1992). To determine whether *GCT* and *CCT* act through the GA pathway, we examined how variation in the amount of GA affects the phenotype of *gct* and *cct*. Exogenously applied GA_3 accelerated abaxial trichome production and flowering in *gct* and *cct*, whereas *ga1-3* – a mutation that blocks GA biosynthesis – further delayed abaxial trichome production and flowering time in these mutants (Table 1; Fig. 3I-K). The observation that *gct* and *cct* do not interfere with the sensitivity of plants to GA suggests that *GCT* and *CCT* regulate vegetative phase change and flowering in parallel to this hormone.

The vegetative phenotype of *gct* and *cct* is similar to that of plants overexpressing miR156, the miRNA that acts as a master regulator of the juvenile-to-adult transition in *Arabidopsis* (Wu and Poethig, 2006). To determine if *GCT* and *CCT* regulate vegetative phase change via miR156, we examined the effect of *gct* and *cct* on the expression of miR156, as well as the expression of direct (*SPL3* and *SPL9*) and indirect (miR172) targets of this miRNA (Wu et al., 2009) (Fig. 4). Northern blot analysis revealed that miR156 levels were approximately twice as high in *gct* and *cct* mutants as in wt plants at 7 d, 14 d and 21 d after germination. miR156 levels decreased steadily in all genotypes, so that at 21 d the amount of miR156 was about half that seen at 7 d. As reported previously, miR156 and miR172 show opposite patterns of accumulation (Wu et al., 2009). In agreement with this, we found that the increased expression of miR156 in *gct* and *cct* was associated with a decrease in the expression of miR172 at 7 d, 14 d and 21 d (Fig. 4A). Similarly, the mRNA levels of the transcription factors *SPL3* and *SPL9*, which are direct targets of miR156, were reduced in both *gct* and *cct* (Fig. 4C), although in the case of *SPL9* this effect was only observed at 21 d. *gct* and *cct* had no significant effect on the expression of miR159, miR161 and miR168 (Fig. 4C). These results suggest that *GCT* and *CCT* specifically regulate miR156, rather than being generally involved in miRNA transcription.

To determine if the increased expression of miR156 in *gct* and *cct* mutants is responsible for their effect on vegetative phase change, we reduced miR156 levels in these mutants using a 35S::MIM156 transgene. This transgene expresses an imperfect miR156 target site, which reduces free miR156 in the cell by sequestering this miRNA in inactive RISC complexes (Franco-Zorrilla et al., 2007). Consistent with previous reports (Wu et al., 2009; Wang et al., 2009), wt plants carrying a single 35S::MIM156 transgene failed to express juvenile leaf traits: they produced abaxial trichomes starting with leaf 1 (instead of leaf 5.5) (Fig. 5A), and all of their rosette leaves had the pattern of leaf serrations (Fig. 5B) and the elongated shape (Fig. 5C) characteristic of adult leaves. 35S::MIM156 had this same effect in the *gct* and *cct* mutant backgrounds: transgenic *gct* and *cct* plants produced abaxial trichomes on leaf 1 (instead of 16 and 15.5, respectively) (Fig. 5A), and had more serrated (Fig. 5B) and more highly elongated (Fig. 5C) leaves than wt plants. Although

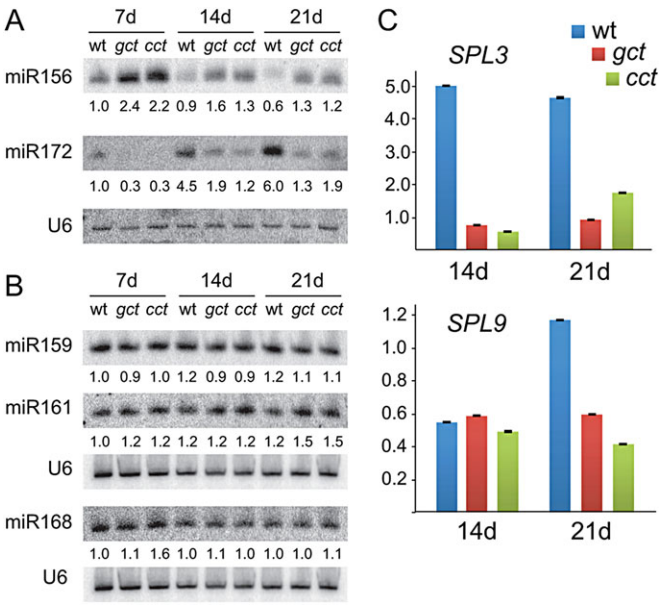

Fig. 4. *GCT* and *CCT* regulate miR156, miR172 and SPL genes. Northern blot and qRT-PCR analysis of 7 d, 14 d and 21 d wt, *gct* and *cct* plants grown in long-day conditions. (A) Northern blot detection of miR156 and miR172. One representative example of three biological replicates is shown. (B) Northern blot detection of miR159, miR161 and miR168. One experiment was performed. (A,B) Intensity values normalized to the *U6* loading control are given beneath each lane. (C) qRT-PCR analysis of *SPL3* and *SPL9* transcript levels, normalized to *EIF4A*. One of two biological replicates is shown. Error bars represent the s.d. of three technical replicates.

Development (2014) 141, 4580-4589 doi:10.1242/dev.111229

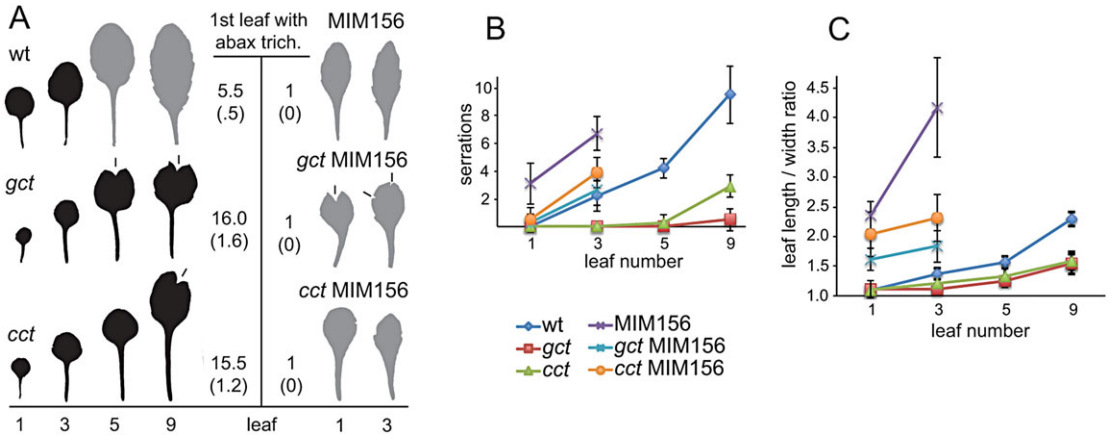

Fig. 5. Decrease in miR156 activity rescues the vegetative phase change phenotype of *gct* and *cct* plants. Phenotypic analysis of leaf shape, serrations and abaxial trichome onset in wt, *gct*, *cct*, MIM156, *gct* MIM156 and *cct* MIM156 plants grown in long-day conditions. (A) Morphology of leaves 1, 3, 5 and 9 (wt, *gct* and *cct*) and of leaves 1 and 3 (MIM156, *gct* MIM156, *cct* MIM156). Leaves with abaxial trichomes are shown in gray, leaves without abaxial trichomes in black. The average position of the first leaf with abaxial trichomes is shown, with s.d. in parentheses. Location of cuts made in leaves in order to flatten them for scanning are indicated with a short line. (B) Number of serrations in leaves 1, 3, 5 and 9 of each genotype. (C) Length-to-width ratios for leaves 1, 3, 5 and 9 of each genotype. Error bars indicate s.d.; $n \geq 12$.

a single copy of 35S::MIM156 was totally epistatic to *gct* and *cct* with regard to abaxial trichome production, it was unable to completely suppress their effect on leaf serrations and the leaf length-to-width ratio. This could mean that the pathways affecting these morphological traits are sensitive to very small amounts of miR156, or that *gct* and *cct* have both miR156-dependent and miR156-independent roles in leaf development.

In summary, these results demonstrate that miR156 is required for the juvenilized phenotype of *gct* and *cct*, and support the conclusion that this phenotype is largely attributable to the increased amount of miR156 in these mutants.

GCT and *CCT* promote the floral transition by repressing *FLC*

gct and *cct* also have a significant effect on the transition to flowering (Fig. 3A). During this transition, the shoot apex produces several flower-bearing branches (co-florescences) subtended by leaves (bracts), and then produces only flowers. In long days, wt plants made an average of 3.1 bracts and flowered 24.7 days after planting (DAP) (Table 1). *gct* plants made an average of 7.2 bracts and flowered 50.8 DAP, while *cct* plants produced an average of 7.8 bracts and flowered 41.3 DAP (Table 1). *gct* and *cct* produced smaller flowers than normal, with occasional fused stamen filaments and a variable number of petals and stamens (Fig. 3B-D; data not shown). *gct* flowers are completely male and female sterile, whereas the flowers of *cct* are initially completely sterile, but will produce a small amount of seed after several months of growth. Thus, as previously reported for *cct* (*crp*) by Imura et al. (2012), *GCT* and *CCT* promote floral induction and also play a role in floral morphogenesis.

Our microarray analysis revealed that the late flowering phenotype of *gct* and *cct* is associated with reduced expression of the floral inducers *FT*, *SOC1*, *SEPALLATA3* (*SEP3*), *FRUITFULL* (*FUL*) and *CO* and with elevated expression of the floral repressor *FLC* (Fig. 6A; supplementary material Tables S2-S4), which is consistent with the known regulatory interactions between these genes (Fig. 6B) (Amasino, 2010). To validate and extend these results, we quantified *FLC*, *FT* and *SOC1* levels in wt, *gct* and *cct* plants at 6 d and 21 d. In wt plants, *FLC* transcripts remained steady at 6 d and 21 d, whereas *SOC1* and *FT* increased dramatically (consistent with the vegetative-to-floral transition having occurred by 21 d) (Fig. 6C,D). In *gct* and *cct* plants, we found that levels of *FLC* transcripts were much higher than in wt at 6 d, and had decreased several fold by 21 d (Fig. 6C), whereas the levels of *FT* and *SOC1* increased slightly from 6 d to 21 d (Fig. 6D,E). These changes in *FT* and *SOC1* gene expression are not attributable to differences in leaf identity between wt, *gct* and *cct*, as *FT* and *SOC1* show essentially the same expression in juvenile and adult leaves (supplementary material Fig. S3). Although *FLC* is expressed more highly in juvenile than in adult leaves (supplementary material Fig. S3), a secondary effect of leaf identity is unlikely to explain the large differences in *FLC* levels between wt, *gct* and *cct* because the largest differences in *FLC* were observed at 6 d, when all three genotypes have only two juvenile leaf primordia (Fig. 3E-H). Thus, *gct* and *cct* mutants show large increases in expression of the floral repressor *FLC*, and, in turn, show decreased expression of the *FLC* targets *FT* and *SOC1*.

As shown in Fig. 4, *gct* and *cct* also have higher levels of miR156, a miRNA that has previously been shown to cause a small delay in flowering in long-day conditions when overexpressed (Wang et al., 2009). This raises the possibility that the increased level of *FLC* in *gct* and *cct* might be attributable to the increased level of miR156 in these mutants (Fig. 4). To test this, we examined *FLC* levels in 35S::miR156A plants and found a ~30% decrease in the level of *FLC* compared with wt (supplementary material Fig. S4). Because *gct* and *cct* show elevated levels of both miR156 and *FLC*, we conclude that the increase in *FLC* in *gct* and *cct* is not caused by the increase in miR156.

To determine whether the late flowering phenotype of *gct* and *cct* is indeed attributable to the increased expression of *FLC*, we crossed the *flc-3* null mutation into *gct* and *cct* mutant backgrounds. The flowering time of these double mutants was intermediate between the two parents: *gct flc-3* double mutants flowered ~7 days earlier than *gct*, while *cct flc-3* double mutants flowered 6 days earlier than *cct* (Table 1; Fig. 6F), but neither genotype flowered as early as *flc-3*. The levels of *FT* and *SOC1* in these double mutants were consistent with their intermediate phenotype. Whereas *flc-3* completely blocked the effect of *cct* on *SOC1* expression in 21 d plants (Fig. 6E), it had only a small effect on *FT* expression in *cct* mutants (Fig. 6D). *flc-3* had little or no effect on the expression of *FT* and *SOC1* in a *gct* mutant background (Fig. 6D,E). This result

Development (2014) 141, 4580-4589 doi:10.1242/dev.111229

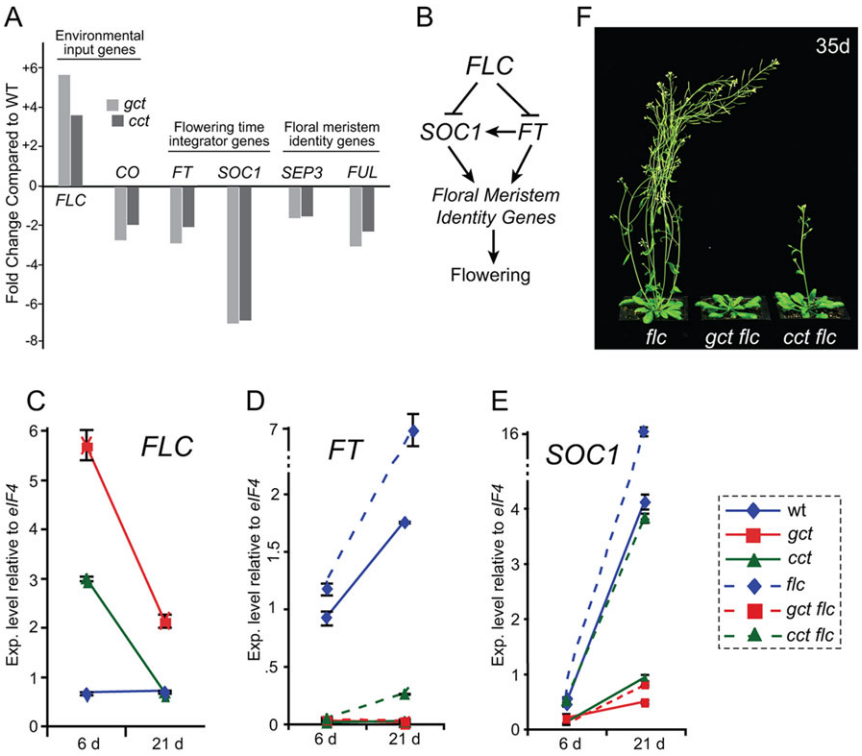

Fig. 6. *GCT* and *CCT* regulate *FLC* and its downstream targets. (A) Affymetrix microarray analysis of *CO*, *FLC* and the *FLC* targets *FT*, *SOC1*, *SEP3* and *FUL* in 9 d *gct* and *cct* seedlings compared with 7 d wt seedlings. (B) Regulatory interactions between *FLC*, *SOC1* and *FT*. (C-E) Expression of *FLC* (C), *FT* (D) and *SOC1* (E) in wt, *gct*, *cct*, *flc-3*, *gct flc-3* and *cct flc-3* plants at 6 d and 21 d. The average of three technical replicates for one representative experiment of two biological replicates is shown. Error bars indicate s.d. Results were normalized to expression of *EIF4A*. (F) *flc-3*, *gct flc-3* and *cct flc-3* 35 d plants. See Fig. 3I for 35 d wt, *gct* and *cct* plants.

indicates that the elevated expression of *FLC* contributes to the late flowering phenotype of *cct* and *gct*, but is not entirely responsible for this phenotype.

DISCUSSION

Multicellular organisms pass through several developmental phases during their life cycle. In *Arabidopsis*, these stages include embryogenesis and seed formation, germination, juvenile and adult phases of vegetative growth, and a reproductive phase that culminates in gamete production and fertilization. We have previously shown that the transcriptional repressors *GCT* (*MED13*) and *CCT* (*MED12*) regulate the timing of pattern formation during *Arabidopsis* embryogenesis (Gillmor et al., 2010). In the current study we show that *GCT* and *CCT* play a global role in the regulation of developmental timing, promoting the seed-to-seedling transition, vegetative phase change, and flowering.

Microarray analysis demonstrated that *GCT* and *CCT* share close to half of their direct or indirect gene targets, with 490 transcripts increasing in both *gct* and *cct* (out of a total 1267 genes increasing in *gct* and 925 in *cct*), and 683 transcripts decreasing in both mutants (out of 1373 genes decreasing in *gct* and 1051 in *cct*). The number of transcripts that change in level is comparable with the findings of RNA profiling in single cell types in *Drosophila* [S2 cells, where a total of 361 genes were found to change in *med12* (*kohtalo*) or *med13* (*skuld*) mutants] and yeast (where a total of 900 genes were found to increase or decrease), as is the highly significant overlap that we observed between the transcripts that change in common between *med12* and *med13* mutants (Kuuluvainen et al., 2014; Van de Peppel et al., 2005). It is commonly accepted that MED12 and MED13 primarily act as transcriptional repressors (Carlsten et al., 2013), and thus many of the transcripts whose steady-state levels decrease in *gct* and *cct* mutants are unlikely to be direct targets of *GCT* and *CCT* regulation. However, there are also reports of the CDK8 module acting as a transcriptional activator (Carrera et al., 2008; Donner et al., 2007). No genome-wide chromatin immunoprecipitation (ChIP) profiling experiment has been reported for either MED12 or MED13 in plants or animals. Despite the challenges inherent in ChIP analysis using such large proteins, determination of the direct targets of MED12 and MED13 is an important goal for future research in both *Arabidopsis* and animals.

In addition to the molecular data discussed above, genetic analysis provides functional evidence that *GCT* and *CCT* regulate many of the same processes. For example, *gct* and *cct* single mutants express either a weak 'grow' phenotype characterized by moderate defects in vegetative and reproductive timing, or a strong 'arrest' phenotype of arrested growth. By contrast, *gct cct* double mutants express only the arrest phenotype. This result suggests that, in the absence of either MED12 or MED13, the CDK8 module is partially functional and can still promote post-embryonic growth, albeit in a less effective manner, leading to the variable expressivity of the *gct* and *cct* grow and arrest phenotypes. This result, and the observation that *gct cct* double mutants only have the severe arrest phenotype, suggest that *GCT* and *CCT* have closely related, but not completely redundant functions. This is consistent with studies of MED12 and MED13 in yeast and animals, where they have been shown to affect transcription of many of the same genes and to have nearly identical mutant phenotypes (Samuelsen et al., 2003; Janody et al., 2003; van de Peppel et al., 2005; Yoda et al., 2005). Additionally, *in vitro* studies have demonstrated that, although MED12 and MED13 are capable of individually blocking transcription, they act most efficiently together (Knuesel et al., 2009).

The CDK8 module of Mediator represses transcription by at least two mechanisms. Structural studies in yeast and humans demonstrate that this module binds Core Mediator, blocking the Core Mediator-RNA polymerase II interaction (Elmlund et al., 2006; Tsai et al., 2013). The MED13, MED12 and CDK8 subunits all contribute to binding, with MED13 playing the most important role, followed by MED12 and CDK8 (Tsai et al., 2013). These results are consistent with the mutant phenotypes of these proteins in *Arabidopsis*, as the expressivity of the growth arrest phenotype is

Development (2014) 141, 4580-4589 doi:10.1242/dev.111229

higher for *gct* (*med13*) than for *cct* (*med12*). Human MED12 also represses gene expression by recruiting H3K9 and H3K27 methylation to target loci through its interaction with the histone methyltransferase G9a (EHMT2) (Ding et al., 2008; Chaturvedi et al., 2009, 2012). Steric hindrance of RNA polymerase II-Core Mediator interactions represents a relatively flexible form of transcriptional repression, whereas H3K9 and H3K27 methylation is likely to have more stable effects on gene expression. The mutant phenotype of the *gct cct* double mutant suggests that both activities are necessary for full repression by the CDK8 module. H3K9 and H3K27 methylation have well-established roles in the seed-to-seedling and vegetative-to-reproductive transitions. The PRC2 complex represses the expression of embryonic genes after germination by recruiting deposition of H3K27 methylation (Bouyer et al., 2011). Likewise, the flowering repressor *FLC* is repressed by both H3K9 and H3K27 marks (Bastow et al., 2004). It will be important to determine whether the effect of *GCT* and *CCT* on these genes is mediated by these histone modifications.

Our results indicate that the delayed vegetative phase change phenotype of *gct* and *cct* is attributable to an increase in the abundance of miR156 and a corresponding decrease in levels of the downstream miRNA miR172. miR156 was elevated in *gct* and *cct* throughout shoot development, and declined at the same time in mutant and wt plants, suggesting that *GCT* and *CCT* might regulate the amplitude, rather than the temporal pattern, of miR156 expression. It will be important to determine if *GCT* and *CCT* directly regulate the transcription of specific MIR156 genes or whether they modulate the transcription of an upstream regulator of one or more MIR156 genes, in order to investigate the molecular mechanism of this effect. Whatever this mechanism might be, it is interesting that the relatively small change in the amount of miR156 in these mutants (~2-fold) has such a drastic effect on the expression of phase-specific traits. This suggests that fine-tuning of MIR156 expression by *GCT* and *CCT* is crucial for normal phase change, and raises the possibility that spatial or temporal variation in the activity of these proteins might contribute to natural variation in the timing of the vegetative phase change. Our results also suggest that *GCT* and *CCT* play an important role in controlling the timing of the vegetative-to-floral transition by direct or indirect regulation of *FLC*, as well as through additional, yet to be determined, pathways. Using physiological and genetic experiments, we demonstrated that *GCT* and *CCT* regulate the seed-to-seedling transition, vegetative phase change and flowering in parallel with the phytohormone GA.

Developmental transitions are characterized by a decrease in the expression of genes that specify the pre-existing developmental phase and by an increase in the expression of genes that promote the subsequent phase. In principle, the decline in gene expression during these transitions could be mediated by the loss of factors that promote gene expression, by the appearance of factors that repress gene expression, or by a combination of these events. The pleiotropic phenotype of *gct* and *cct* implies that active transcriptional repression by GCT (MED13) and CCT (MED12) plays a major role during many temporal transitions in *Arabidopsis*. This paradigm has been established for a few developmental transitions in *Arabidopsis* – the best example being the repression of *FLC* expression during vernalization – but the generality of transcriptional repression as a mechanism for developmental transition had not been fully appreciated until now. Our results demonstrate that *GCT* and *CCT* are not required for the downregulation of gene expression during phase transitions per se, but rather for the magnitude and perhaps the stability of the repressed state. It is reasonable to assume that they perform this function in association with temporally regulated transcription factors, and a major challenge for the future is to identify these transcription factors and the ways in which they interact with *GCT* and *CCT* to repress gene expression.

MATERIALS AND METHODS

Genetic stocks and growth conditions

All seed stocks were in the Columbia ecotype. Seeds were sown on soil (Farfard #2) and placed at 4°C for 3 days, before moving flats to growth chambers or laboratory growth racks under 16 h fluorescent illumination (140 µmol/m^2/s) at 22°C. Days to first open flower were measured beginning on the day flats were placed in the growth chamber. For GA treatments, plants were sprayed daily with 100 µM GA_3 (Sigma-Aldrich). For the microarray experiments, plants were grown under long-day conditions (16 h light:8 h dark; 100-125 µmol/m^2/s) in a Conviron growth chamber at a constant 23°C under a 1:1 ratio of T8 Sylvania Octron 4100K Ecologic and GroLite WS fluorescent lamps (Interlectric).

The reference alleles *gct-2* (ABRC stock CS65889; referred to as *gct* throughout the paper) and *cct-1* (ABRC stock CS65890; referred to as *cct* throughout the paper) described by Gillmor et al. (2010) were used for all analyses. The *gct-2* mutation was genotyped using the *gct-2* dCAPS primer pair, and the *cct-1* mutation was genotyped using the *cct-1* dCAPS primer pair. dCAPS primers were designed using dCAPS Finder 2.0 (Neff et al., 2002; http://helix.wustl.edu/dcaps/). The *ga1-3* allele, originally in the L*er* ecotype (Wilson et al., 1992), was introgressed six times into the Col ecotype, and was genotyped based on its morphological phenotype. The *flc-3* allele was used for analysis of the *FLC* gene (Michaels and Amasino, 1999). *flc-3* mutants were genotyped using the *flc-3* primer pair. The *35S::MIM156* target mimicry line for miR156 was genotyped based on its morphological phenotype (Franco-Zorrilla et al., 2007). Sequences of genotyping primers are listed in supplementary material Table S1.

RNA expression analyses

The microarray experiment was performed on three biological replicates of 7 d wt and 9 d *gct* and *cct* mutants with the 'grow' phenotype, each replicate being a pool of at least 20 seedlings. Different time points were used because they were when the first two leaf primordia of these three genotypes were 1 mm in length. Total RNA was extracted with TRI Reagent (Sigma-Aldrich), and further purified using RNeasy columns (Qiagen) with on-column DNase treatment (Qiagen). Biotin-labeled cDNA targets for hybridization to Affymetrix *Arabidopsis* ATH1 microarrays were prepared essentially as described by Willmann et al. (2011). The University of Pennsylvania Microarray Core Facility hybridized the arrays. Raw data have been deposited at Gene Expression Omnibus under accession number GSE56155.

The microarrays were gcRMA normalized in R (http://www.r-project.org/) and filtered using MAS5.0 presence/absence calls to remove any probe sets not expressed in at least three samples. The remaining 16,826 non-control probe sets were tested for differential expression in R using Limma (Bioconductor) with contrast and a Benjamini-Hochberg multiple test correction (MTC), $P \leq 0.05$. Enrichment of GO terms, SP_PIR keywords, PIR Superfamilies, and SMART, INTERPRO, COG_ONTOLOGY and UP_SEQ features within the lists of probe sets increasing and decreasing in both *gct* and *cct* was performed using DAVID Bioinformatics Resources 6.7 (http://david.abcc.ncifcrf.gov/home.jsp; Dennis et al., 2003; Huang et al., 2009) with the 16,826 expressed probe sets as a background. The probe sets differentially expressed in both *gct* and *cct* were also compared with the 862 probe sets shown to specifically increase in green cotyledon stage embryos by Willmann et al. (2011) (Cluster 9).

For quantitative RT-PCR (qRT-PCR), total RNA was isolated as described above for ten pooled seedlings per time point, per biological replicate. Reverse transcription was performed with the oligo(dT)$_{20}$ primer using the SuperScript II First-Strand Synthesis System for RT-PCR (Invitrogen). Quantitative PCR was performed with Fast SYBR Green Master Mix (Applied Biosystems) on a StepOnePlus RT-PCR System (Applied Biosystems). Transcript levels were normalized against *EUKARYOTIC TRANSLATION INITIATION FACTOR 4A* (*EIF4A*). Primers for qRT-PCR were designed using AtRTPrimer (http://pbil.kaist.ac.kr/AtRTPrimer; Han and Kim, 2006) and are listed in supplementary material Table S1.

Development (2014) 141, 4580-4589 doi:10.1242/dev.111229

For small RNA northern blots, 30 µg total RNA was separated on 8 M urea/15% denaturing polyacrylamide gels and electrically transferred to a Hybond-N+ nylon membrane (GE Healthcare). Blots were hybridized with [γ-^{32}P]ATP-labeled complementary oligonucleotide probes for 3 h at 40°C in Rapid-hyb hybridization buffer (GE Healthcare). A *U6* RNA-complementary oligonucleotide probe was used as a loading control. Blots were washed twice at 40°C in 5×SSC, 0.1% SDS for 20 min, and were scanned with a Storm 820 phosphorimager (Amersham Biosciences). Oligonucleotide probes used are listed in supplementary material Table S1. Signal intensities were quantified using ImageJ (NIH).

Morphological and histological analyses

Analysis of leaf traits, such as size, shape and the presence of abaxial trichomes, was performed at ~4 weeks in order to allow leaves to reach their final size. The presence of abaxial trichomes was scored using a dissecting microscope. Leaf length and width ratios, as well as the number of serrations, were quantified by taping leaves to paper, scanning and analyzing in Photoshop (Adobe).

Acknowledgements

We thank Keith Earley and Enrique Ibarra-Laclette for advice on qRT-PCR, and Doris Wagner and Kimberly Gallagher for helpful discussions during the course of this study.

Competing interests

The authors declare no competing financial interests.

Author contributions

C.S.G., M.R.W., M.B.-M. and R.S.P. designed experiments. C.S.G., C.O.S.-O. and M.B.-M. performed all experiments, with the exception of the microarray experiments and analysis, which were performed by M.R.W. All authors analyzed data. C.S.G. and R.S.P. wrote the manuscript, with input from the other authors.

Funding

This work was funded by a US Department of Energy (DOE) grant to R.S.P. and C.S.G. [DE-FG02-99ER20328], a National Institutes of Health (NIH) grant [RO1 GM51893] to R.S.P., an NIH NRSA postdoctoral fellowship to C.S.G. [F32 GM069104], an NIH NRSA postdoctoral fellowship to M.R.W. [F32 GM075540], a CONACyT PhD fellowship to M.B.-M. [No. 326677], CINVESTAV institutional funds, and by a CONACyT grant to C.S.G. [No. 152333]. Deposited in PMC for release after 12 months.

Supplementary material

Supplementary material available online at
http://dev.biologists.org/lookup/suppl/doi:10.1242/dev.111229/-/DC1

References

Abedon, B. G., Hatfield, R. D. and Tracy, W. F. (2006). Cell wall composition in juvenile and adult leaves of maize (*Zea mays* L.). *J. Agric. Food Chem.* **54**, 3896-3900.

Amasino, R. (2010). Seasonal and developmental timing of flowering. *Plant J.* **61**, 1001-1013.

Aukerman, M. J. and Sakai, H. (2003). Regulation of flowering time and floral organ identity by a microRNA and its APETALA2-like target genes. *Plant Cell* **15**, 2730-2741.

Bassel, G. W., Lan, H., Glaab, E., Gibbs, D. J., Gerjets, T., Krasnogor, N., Bonner, A. J., Holdsworth, M. J. and Provart, N. J. (2011). Genome-wide network model capturing seed germination reveals coordinated regulation of plant cellular phase transitions. *Proc. Natl. Acad. Sci. USA* **108**, 9709-9714.

Bastow, R., Mylne, J. S., Lister, C., Lippman, Z., Martienssen, R. A. and Dean, C. (2004). Vernalization requires epigenetic silencing of *FLC* by histone methylation. *Nature* **427**, 164-167.

Boege, K. and Marquis, R. J. (2005). Facing herbivory as you grow up: the ontogeny of resistance in plants. *Trends Ecol. Evol.* **20**, 441-448.

Bourbon, H.-M. (2008). Comparative genomics supports a deep evolutionary origin for the large, four-module transcriptional mediator complex. *Nucleic Acids Res.* **36**, 3993-4008.

Bouyer, D., Roudier, F., Heese, M., Andersen, E. D., Gey, D., Nowack, M. K., Goodrich, J., Renou, J.-P., Grini, P. E., Colot, V. et al. (2011). Polycomb repressive complex 2 controls the embryo-to-seedling phase transition. *PLoS Genet.* **7**, e1002014.

Carlsten, J. O. P., Zhu, X. and Gustafsson, C. M. (2013). The multitalented Mediator complex. *Trends Biochem. Sci.* **38**, 531-537.

Carrera, I., Janody, F., Leeds, N., Duveau, F. and Treisman, J. E. (2008). Pygopus activates Wingless target gene transcription through the mediator complex subunits Med12 and Med13. *Proc. Natl. Acad. Sci. USA* **105**, 6644-6649.

Chandler, M. A., Riedeman, E. S. and Tracy, W. F. (2011). Vegetative phase change in maize: biotic resistance and agronomic performance. *Plant Breed. Rev.* **34**, 131-160.

Chaturvedi, C.-P., Hosey, A. M., Palii, C., Perez-Iratxeta, C., Nakatani, Y., Ranish, J. A., Dilworth, F. J. and Brand, M. (2009). Dual role for the methyltransferase G9a in the maintenance of β-globin gene transcription in adult erythroid cells. *Proc. Natl. Acad. Sci. USA* **106**, 18303-18308.

Chaturvedi, C.-P., Somasundaram, B., Singh, K., Carpenedo, R. L., Stanford, W. L., Dilworth, F. J. and Brand, M. (2012). Maintenance of gene silencing by the coordinate action of the H3K9 methyltransferase G9a/KMT1C and the H3K4 demethylase Jarid1a/KDM5A. *Proc. Natl. Acad. Sci. USA* **109**, 18845-18850.

Chien, J. C. and Sussex, I. M. (1996). Differential regulation of trichome formation on the adaxial and abaxial leaf surfaces by gibberellins and photoperiod in *Arabidopsis thaliana* (L.) Heynh. *Plant Physiol.* **111**, 1321-1328.

Chuck, G., Cigan, A. M., Saeteurn, K. and Hake, S. (2007). The heterochronic maize mutant Corngrass1 results from overexpression of a tandem microRNA. *Nat. Genet.* **39**, 544-549.

Crevillén, P. and Dean, C. (2011). Regulation of the floral repressor gene *FLC*: the complexity of transcription in a chromatin context. *Curr. Opin. Plant Biol.* **14**, 38-44.

Dennis, G., Sherman, B. T., Hosack, D. A., Yang, J., Gao, W., Lane, H. C. and Lempicki, R. A. (2003). DAVID: Database for Annotation, Visualization, and Integrated Discovery. *Genome Biol.* **4**, P3.

Ding, N., Zhou, H., Esteve, P.-O., Chin, H. G., Kim, S., Xu, X., Joseph, S. M., Friez, M. J., Schwartz, C. E., Pradham, S. et al. (2008). Mediator links epigenetic silencing of neuronal gene expression with x-linked mental retardation. *Mol. Cell* **31**, 347-359.

Donner, A. J., Szostek, S., Hoover, J. M. and Espinosa, J. M. (2007). CDK8 is a stimulus-specific positive coregulator of p53 target genes. *Mol. Cell* **27**, 121-133.

Elmlund, H., Baraznenok, V., Lindahl, M., Samuelsen, C. O., Koeck, P. J. B., Holmberg, S., Hebert, H. and Gustafsson, C. M. (2006). The cyclin-dependent kinase 8 module sterically blocks Mediator interactions with RNA polymerase II. *Proc. Natl. Acad. Sci. USA* **103**, 15788-15793.

Evans, M. M. S. and Poethig, R. S. (1995). Gibberellins promote vegetative phase change and reproductive maturity in maize. *Plant Physiol.* **108**, 475-487.

Franco-Zorrilla, J. M., Valli, A., Todesco, M., Mateos, I., Puga, M. I., Rubio-Somoza, I., Leyva, A., Weigel, D., García, J. A. and Paz-Ares, J. (2007). Target mimicry provides a new mechanism for regulation of microRNA activity. *Nat. Genet.* **39**, 1033-1037.

Geuten, K. and Coenen, H. (2013). Heterochronic genes in plant evolution and development. *Front. Plant Sci.* **4**, 381.

Gillmor, C. S., Park, M. Y., Smith, M. R., Pepitone, R., Kerstetter, R. A. and Poethig, R. S. (2010). The MED12-MED13 module of Mediator regulates the timing of embryo patterning in Arabidopsis. *Development* **137**, 113-122.

Gould, S. J. (1977). *Ontogeny and Phylogeny*. Cambridge, MA, USA: Belknap Press of Harvard University Press.

Han, S. and Kim, D. (2006). AtRTPrimer: database for Arabidopsis genome-wide homogeneous and specific RT-PCR primer-pairs. *BMC Bioinformatics* **7**, 179.

Huang, D. W., Sherman, B. T. and Lempicki, R. A. (2009). Systematic and integrative analysis of large gene lists using DAVID bioinformatics resources. *Nat. Protoc.* **4**, 44-57.

Huijser, P. and Schmid, M. (2011). The control of developmental phase transitions in plants. *Development* **138**, 4117-4129.

Imura, Y., Kobayashi, Y., Yamamoto, S., Furutani, M., Tasaka, M., Abe, M. and Araki, T. (2012). *CRYPTIC PRECOCIOUS/MED12* is a novel flowering regulator with multiple target steps in Arabidopsis. *Plant Cell Physiol.* **53**, 287-303.

Ito, J., Sono, T., Tasaka, M. and Furutani, M. (2011). *MACCHI-BOU2* is required for early embryo patterning and cotyledon organogenesis in Arabidopsis. *Plant Cell Physiol.* **52**, 539-552.

Janody, F., Martirosyan, Z., Benlali, A. and Treisman, J. E. (2003). Two subunits of the Drosophila Mediator complex act together to control cell affinity. *Development* **130**, 3691-3701.

Kim, Y. J., Zheng, B., Yu, Y., Won, S. Y., Mo, B. and Chen, X. (2011). The role of Mediator in small and long noncoding RNA production in *Arabidopsis thaliana*. *EMBO J.* **30**, 814-822.

Knuesel, M. T., Meyer, K. D., Bernecky, C. and Taatjes, D. J. (2009). The human CDK8 subcomplex is a molecular switch that controls Mediator coactivator function. *Genes Dev.* **23**, 439-451.

Koornneef, M. and van der Veen, J. H. (1980). Induction and analysis of Gibberellin sensitive mutants in *Arabidopsis thaliana* (L.) Heynh. *Theoret. Appl. Genet.* **58**, 257-263.

Kuuluvainen, E., Hakala, H., Havula, E., Estimé, M. S., Rämet, M., Hietakangas, V. and Mäkelä, T. P. (2014). Cyclin-dependent kinase 8 module expression profiling reveals requirement of Mediator subunits 12 and 13 for transcription of Serpent-dependent innate immunity genes in Drosophila. *J. Biol. Chem.* **289**, 16252-16261.

Lai, Z., Schluttenhofer, C. M., Bhide, K., Shreve, J., Thimmapuram, J., Lee, S. Y., Yun, D.-J. and Mengiste, T. (2014). MED18 interaction with distinct transcription factors regulates multiple plant functions. *Nat. Commun.* **5**, 3064.

Michaels, S. D. and Amasino, R. M. (1999). *FLOWERING LOCUS C* encodes a novel MADS domain protein that acts as a repressor of flowering. *Plant Cell* **11**, 949-956.
Neff, M. M., Turk, E. and Kalishman, M. (2002). Web-based primer design for single nucleotide polymorphism analysis. *Trends Genet.* **18**, 613-615.
Nemet, J., Jelicic, B., Rubelj, I. and Sopta, M. (2013). The two faces of Cdk8, a positive/negative regulator of transcription. *Biochimie* **97**, 22-27.
Ogas, J., Cheng, J.-C., Sung, Z. R. and Somerville, C. (1997). Cellular differentiation regulated by gibberellin in the *Arabidopsis thaliana* pickle mutant. *Science* **277**, 91-94.
Poethig, R. S. (2013). Vegetative phase change and shoot maturation in plants. *Curr. Top. Dev. Biol.* **105**, 125-152.
Röbbelen, G. (1957). Uber heterophyllie bei *Arabidopsis thaliana* (L.). *Heynh Berichte der Deutschen Botanischen Gesellschaft* **70**, 39-44.
Samuelsen, C. O., Baraznenok, V., Khorosjutina, O., Spahr, H., Kieselbach, T., Holmberg, S. and Gustafsson, C. M. (2003). TRAP230/ARC240 and TRAP240/ARC250 Mediator subunits are functionally conserved through evolution. *Proc. Natl. Acad. Sci. USA* **100**, 6422-6427.
Schmid, M., Davison, T. S., Henz, S. R., Pape, U. J., Demar, M., Vingron, M., Schölkopf, B., Weigel, D. and Lohmann, J. U. (2005). A gene expression map of *Arabidopsis thaliana* development. *Nat. Genet.* **37**, 501-506.
Telfer, A., Bollman, K. M. and Poethig, R. S. (1997). Phase change and the regulation of trichome distribution in *Arabidopsis thaliana*. *Development* **124**, 645-654.
Tsai, K.-L., Sato, S., Tomomori-Sato, C., Conaway, R. C., Conaway, J. W. and Asturias, F. J. (2013). A conserved Mediator-CDK8 kinase module association regulates Mediator-RNA polymerase II interaction. *Nat. Struct. Mol. Biol.* **20**, 611-619.
van de Peppel, J., Kettelarij, N., van Bakel, H., Kockelkorn, T. T. J. P., van Leenen, D. and Holstege, F. C. P. (2005). Mediator expression profiling epistasis reveals a signal transduction pathway with antagonistic submodules and highly specific downstream targets. *Mol. Cell* **19**, 511-522.
Wang, W. and Chen, X. (2004). *HUA ENHANCER3* reveals a role for a cyclin-dependent protein kinase in the specification of floral organ identity in Arabidopsis. *Development* **131**, 3147-3156.
Wang, J.-W., Czech, B. and Weigel, D. (2009). miR156-regulated *SPL* transcription factors define an endogenous flowering pathway in Arabidopsis thaliana. *Cell* **138**, 738-749.
Willmann, M. R., Mehalick, A. J., Packer, R. L. and Jenik, P. D. (2011). MicroRNAs regulate the timing of embryo maturation in Arabidopsis. *Plant Physiol.* **155**, 1871-1884.
Wilson, R. N., Heckman, J. W. and Somerville, C. R. (1992). Gibberellin is required for flowering in *Arabidopsis thaliana* under short days. *Plant Physiol.* **100**, 403-408.
Winter, D., Vinegar, B., Nahal, H., Ammar, R., Wilson, G. V. and Provart, N. J. (2007). An 'Electronic Fluorescent Pictograph' browser for exploring and analyzing large-scale biological data sets. *PLoS ONE* **2**, e718.
Wu, G. and Poethig, R. S. (2006). Temporal regulation of shoot development in Arabidopsis thaliana by miR156 and its target *SPL3*. *Development* **133**, 3539-3547.
Wu, G., Park, M. Y., Conway, S. R., Wang, J.-W., Weigel, D. and Poethig, R. S. (2009). The sequential action of miR156 and miR172 regulates developmental timing in Arabidopsis. *Cell* **138**, 750-759.
Yang, L., Conway, S. R. and Poethig, R. S. (2011). Vegetative phase change is mediated by a leaf-derived signal that represses the transcription of miR156. *Development* **138**, 245-249.
Yang, L., Xu, M., Koo, Y., He, J. and Poethig, R. S. (2013). Sugar promotes vegetative phase change in *Arabidopsis thaliana* by repressing the expression of *MIR156A* and *MIR156C*. *eLife* **2**, e00260.
Yin, Y.-w. and Wang, G. (2014). The Mediator complex: a master coordinator of transcription and cell lineage development. *Development* **141**, 977-987.
Yoda, A., Kouike, H., Okano, H. and Sawa, H. (2005). Components of the transcriptional Mediator complex are required for asymmetric cell division in *C. elegans*. *Development* **132**, 1885-1893.
Yu, S., Galvão, V. C., Zhang, Y.-C., Horrer, D., Zhang, T.-Q., Hao, Y.-H., Feng, Y.-Q., Wang, S., Schmid, M. and Wang, J.-W. (2012). Gibberellin regulates the Arabidopsis floral transition through miR156-targeted *SQUAMOSA PROMOTER BINDING-LIKE* transcription factors. *Plant Cell* **24**, 3320-3332.
Yu, S., Cao, L., Zhou, C.-M., Zhang, T.-Q., Lian, H., Sun, Y., Wu, J., Huang, J., Wang, G. and Wang, J.-W. (2013). Sugar is an endogenous cue for juvenile-to-adult phase transition in plants. *eLife* **2**, e00269.
Zhang, H., Rider, S. D., Henderson, J. T., Fountain, M., Chuang, K., Kandachar, V., Simons, A., Edenberg, H. J., Romero-Severson, J., Muir, W. M. et al. (2008). The CHD3 remodeler PICKLE promotes trimethylation of histone H3 lysine 27. *J. Biol. Chem.* **283**, 22637-22648.

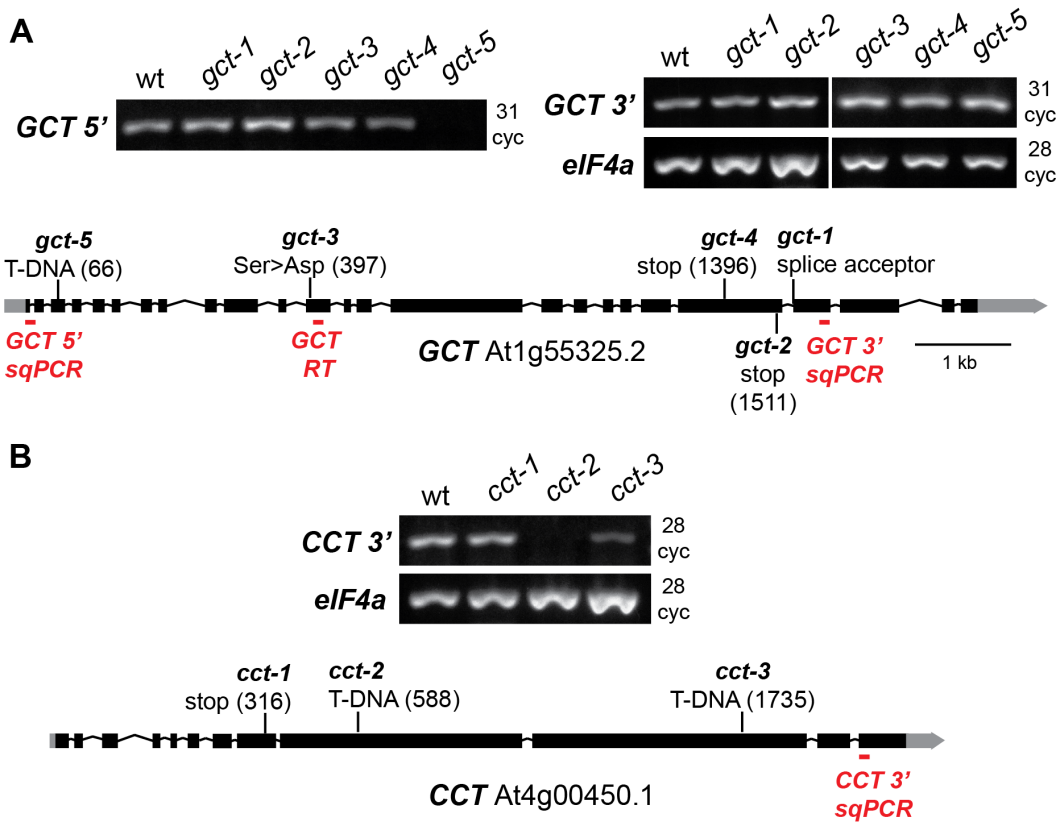

Figure S1. Semi-quantitative RT-PCR analysis of *GCT* and *CCT* transcripts in all *gct* and *cct* alleles, and location of all *gct* and *cct* mutations.

(A) *Above left,* Semi-quantitative RT-PCR analysis of all *gct* alleles detected no *GCT* transcript in *gct-5,* as previously demonstrated by Ito et al. (2011). A primer pair at the 5' end of the transcript (GCT 5' sqPCR, shown in red below) was used to amplify from cDNA generated with a *GCT*-specific RT primer (GCT RT, shown in red below). The *GCT*-specific primer was used for RT because the 5' *GCT* primer pair did not amplify transcript from any wt or *gct* allele using cDNA transcribed with oligo dT, probably due to the 6 kb length of the *GCT* transcript (data not shown). Since the cDNA pool was specific to *GCT*, an eIF4a positive control could not be performed. *Above right*, semi-quantitative RT-PCR analysis of all *gct* alleles using a primer pair in the 3' region of the *GCT* transcript (GCT 3' sqPCR, shown in red below), as well as a primer pair for eIF4a as a control, to amplify from oligo dT cDNA pools. The 5' and 3' *GCT* primer pairs amplify both At1g55325.1 and At1g55325.2 splice variants. *Below*, gene model for *GCT* transcript At1g55325.2. The codon location for all *gct* mutations from Gillmor et al. (2010) are indicated in parentheses, with the exception of *gct-1*, which consists of a G>A change 14bp upstream of the splice acceptor for exon 22, creating an early splice acceptor that results in a downstream frameshift. *gct-5* corresponds to the T-DNA allele SAIL_1169_H11, and also to *mab2-2* (Ito et al., 2011). All other *gct* alleles were generated by EMS mutagenesis (Gillmor et al., 2010).

(B) *Above*, Semi-quantitative RT-PCR analysis detected no *CCT* transcript in *cct-2*, as previously demonstrated by Imura et al. (2012), and greatly reduced transcript levels in *cct-3*. A primer pair in the 3' region of the CCT transcript (*CCT* 3' sqPCR shown in red below) was used to amplify from oligo dT-primed cDNA pools. *Below*, gene model for *CCT* transcript At1g00450.1. The locations of mutations or insertions in all *cct* alleles reported in Gillmor et al. (2010) are shown. The codon locations differ significantly from those in the computationally predicted *CCT* gene model used as a reference in Gillmor et al. (2010). The gene model shown here is based on a cloned *CCT/CRP* cDNA, published by Imura et al. (2012). Importantly, the experimentally determined cDNA sequence demonstrates that the *cct-1* allele causes a translational stop at codon 316, not a Gly>Asp change as predicted by the non-experimentally verified *CCT* transcript model used in Gillmor et al. (2010). *cct-2* corresponds to T-DNA allele SALK_108241, and also to *crp-3* (Imura et al., 2012), while *cct-3* corresponds to T-DNA allele SALK_124276, and also to *crp-4* (Imura et al., 2012).

GCT and *CCT* gene models were drawn based on annotations at www.arabidopsis.org. For all RT-PCR experiments, representative results for one of three biological replicates are shown. RNA was extracted from pools of at least 5 four-week-old plants.

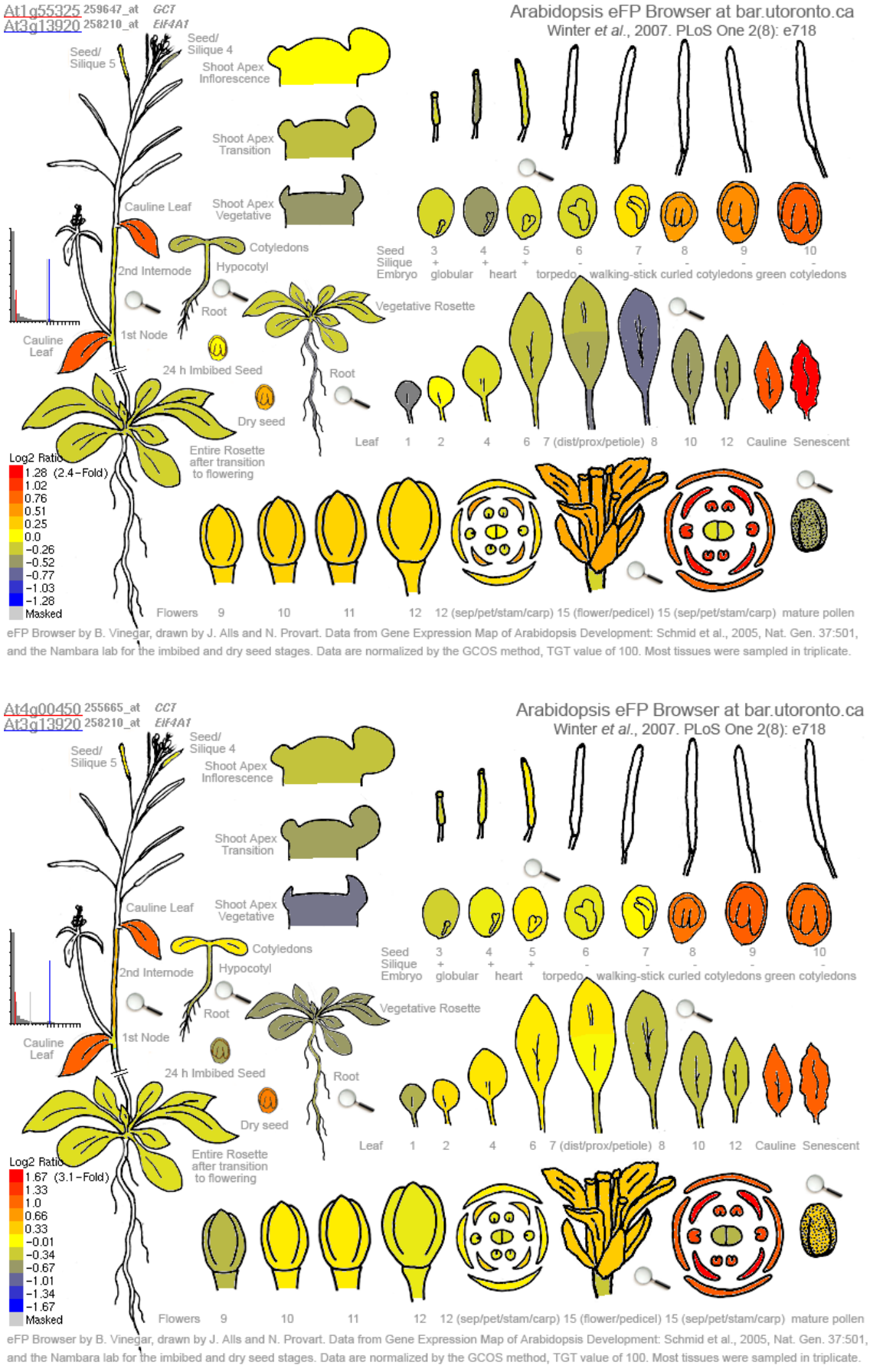

Figure S2. Expression of *GCT* (top) and *CCT* (bottom) relative to *EIF4A*, throughout development. Analysis done with the BAR eFP expression browser (http://bar.utoronto.ca/efp/cgi-bin/efpWeb.cgi).

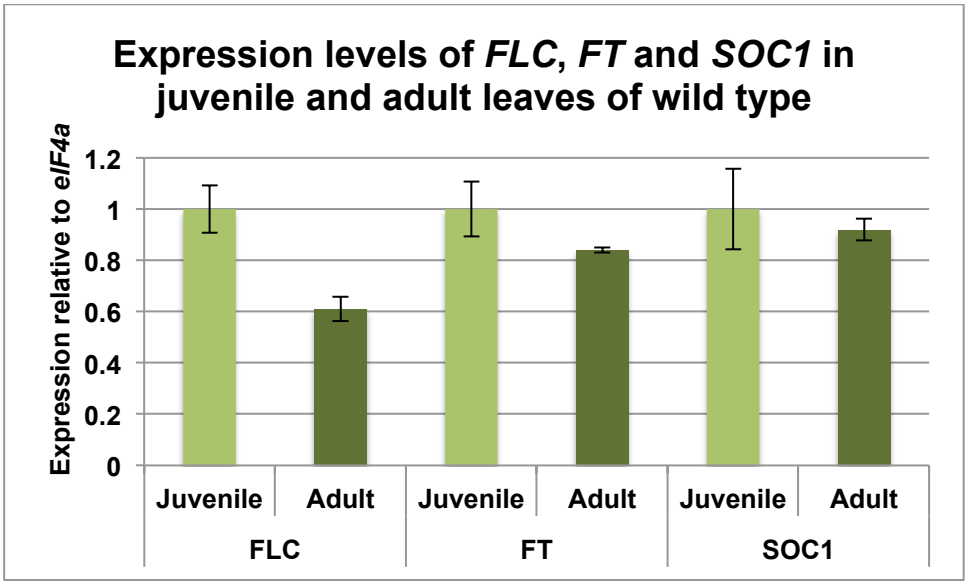

Figure S3. Expression of *FLC, FT* and *SOC1* in juvenile and adult leaves of wild type. Quantitative RT-PCR analysis of *FLC, FT*, and *SOC1* expression in juvenile and adult leaves of 20d old plants grown in long day conditions (see Methods). RNA was extracted from pools of the first three leaves (Juvenile) or the fifth to seventh leaves (Adult) of at least four plants for each biological replicate. Data are the average of three biological replicates, with three technical replicates for each biological replicate. Standard deviation for each average is shown with bars. *eIF4a* was used as a control for expression levels.

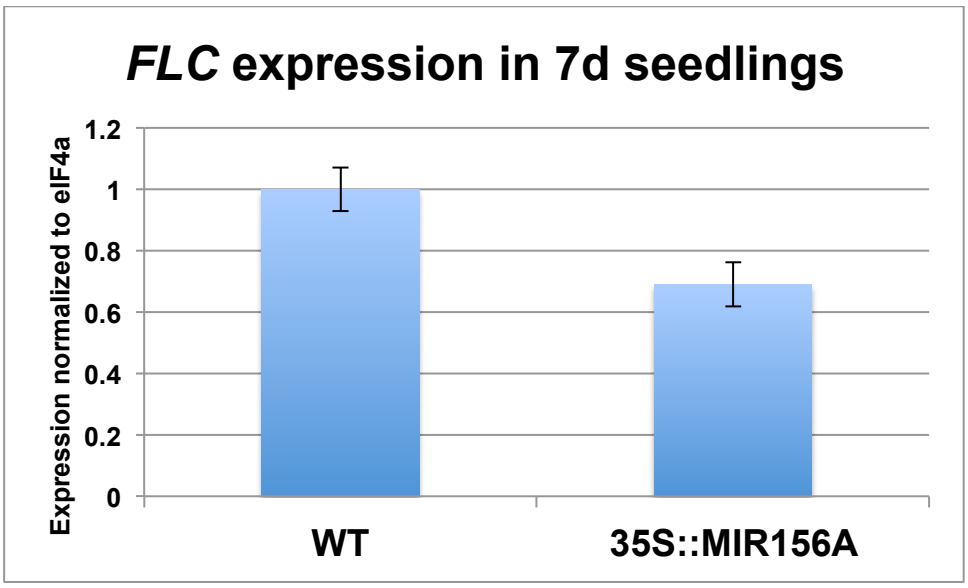

Figure S4. Overexpression of miR156 causes a decrease in *FLC* levels.
Quantitatitve RT-PCR analysis of *FLC* expression in 7d wild type and 35S::MIR156A seedlings. Seedlings were grown in long day conditions (see Methods). The 35S::MIR156A transgenic line is described in Wu and Poethig (2006). Data are the average of three biological replicates, with three technical replicates for each biological replicate. Standard deviation is shown.

Table S1. Sequences of oligonucleotides used in this study			
Name	Sequence (5′ to 3′)	Purpose	Notes
gct-2F	actggagatggcttgtaagcatccg	genotype *gct-2* allele	amplification produces a 200bp product; the wt Col allele is cut at bp 175 by HpaII; the *gct-2* allele does not cut. 50^0C annealing temperature; 3mM $MgCl_2$.
gct-2R	tcgaagaaattcccaatgcg		
cct-1F	agtccagcatcaacaagcc	genotype *cct-1* allele	amplification produces a 125bp product; *cct-1* allele is cut at bp 105 by EcoRV; wt Col allele does not cut. 50^0C annealing temperature; 3mM $MgCl_2$.
cct-1R	actgtagaagacgcaccagata		
flc-3F	gctcgtcatgcggtacacgtg	genotype *flc-3* allele	Amplify a 460bp fragment from wt Col, and a 356 bp fragment from *flc-3*.
flc-3R	ggcgtacttatcgccggagg		
GCT 5' sqPCR F	AATTCCGAGCGCTTCAAGAC	detect transcript in gct alleles at 5' region	
GCT 5' sqPCR R	TGTAGACCACCAATTCTGAAAAC		
GCT 3' sqPCR F	GGTACTCCAAGGGGATTGTTTCAG	detect transcript in gct alleles at 3' region	
GCT 3' sqPCR R	ACCAGCGGATACCAACTCA		
GCT RT	GCATCAGCGTCAAGATCACCAGTT	Reverse transcription with GCT-specific primer	
CCT 3' sqPCR F	GAGCTTACAGAATGAGCTTTCGC	detect transcript in cct alleles at 3' region	
CCT 3' sqPCR R	GAACAGAATGAGGCTGGCATGAGA		
miR156	GTGCTCACTCTCTTCTGTCA	miRNA Northern blot	
miR172	ATGCAGCATCATCAAGATTCT	miRNA Northern blot	
miR159	TAGAGCTCCCTTCAATCCAAA	miRNA Northern blot	
miR161	ACCCCGATGTAGTCACTTTCA	miRNA Northern blot	
miR168	TTCCCGACCTGCACCAAGCGA	miRNA Northern blot	
U6	AGGGGCCATGCTAATCTTCTC	*U6* miRNA Northern blot	

SPL3-F	CTTAGCTGGACACAACGAGAGAAGGC	qRT-PCR	
SPL3-R	GAGAAACAGACAGAGACACAGAGGA	qRT-PCR	
SPL9-F	CAAGGTTCAGTTGGTGGAGGA	qRT-PCR	
SPL9-R	TGAAGAAGCTCGCCATGTATTG	qRT-PCR	
FLC-F	GCCAAGAAGACCGAACTCATGTTGA	qRT-PCR	
FLC-R	TCCAGCAGGTGACATCTCCATCTC	qRT-PCR	
FT-F	TGGTGGATCCAGATGTTCCAAGTC	qRT-PCR	
FT-R	CTCATTGCCAAAGGTTGTTCCAGTT	qRT-PCR	
SOC1-F	GGAGCTGCAACAGATTGAGCAACAG	qRT-PCR	
SOC1-R	CGCTTTCATGAGATCCCCACTTTTC	qRT-PCR	
At2S2-F	ACCCCATGGGCCCAAGACAGA	qRT-PCR	
At2S2-R	GCTGGGGGCCTTGTGGGTTC	qRT-PCR	
CRU1-F	CTCCTTTGCACGTTACATCATCGAG	qRT-PCR	
CRU1-R	CGCATCCAGGGATCACTTTTCC	qRT-PCR	
OLEO1-F	CATCACAGTTGCACTCCTCATCACC	qRT-PCR	
OLEO1-R	TTGCACTGTCCAACTTGTCTGATCC	qRT-PCR	
ATTI7-F	GCCATCTTTTTCATCCTCGTTTTGG	qRT-PCR	
ATTI7-R	CGGGAATATTCGAGGTGCACAGTAG	qRT-PCR	
EIF4aF	AAACTCAATGAAGTACTTGAGGGAC	qRT-PCR	
EIF4aR	TCTCAAAACCATAAGCATAAATACCC	qRT-PCR	

Table S2

Click here to Download Table S2

Table S3

Click here to Download Table S3

Table S4

Click here to Download Table S4

Table S5

Click here to Download Table S5